Traffic Equations

Candidate numbers: 10020,10034,10051,10065

May 23, 2019

Introduction

The traffic equations proposed by Kerner and Konhäuser [1] describes traffic flow and how the traffic on a road behaves when we have flux onto the road from an on-ramp. The equations are given by

$$\rho_t + (\rho v)_x = q(t)\phi(x), \tag{1}$$

$$\rho(v_t + vv_x) = \frac{\rho}{\tau}(V(\rho) - v) - c_0^2\rho_x + \mu v_{xx}, \tag{2}$$

where $\rho(x,t)$ is the local density of vehicles and $v(x,t)$ is the local velocity. In (1), $q(t)\phi(x)$ is the term representing flux onto the road from the on-ramp. We have that $q(t)$ denotes the total incoming flux, while $\phi(x)$ is the spatial distribution of the flux, centered around $x = 0$. Further, in (2), $V(\rho)$ is the safe velocity we have when the traffic flow is homogeneous. The first term on the right hand side ensures that the velocity of the vehicles always will adapt to this safe velocity. The second term on the right hand side takes into account that vehicles have to slow down due to the traffic in front. The last term is a dampening effect needed to fit experimental data.

Implementation

We have chosen to vectorize our equations in order to only handle one equation with our discretization methods. We have also divided the equation into four terms, where $\boldsymbol{u}$ contains all the terms that have been differentiated with respect to the time, $\boldsymbol{F}$ or $\boldsymbol{F_2}$ differentiated with respect to space, $\boldsymbol{s}$ is source/sink-terms and $\boldsymbol{g}$ or $\boldsymbol{g_2}$ are all the other terms not fitting any of the above descriptions. Thus we have the following equation:

$$\frac{\partial \boldsymbol{u}}{\partial t} = -\frac{\partial \boldsymbol{F}(\boldsymbol{u})}{\partial x} + \boldsymbol{g}(\boldsymbol{u}) + \boldsymbol{s}(\boldsymbol{u}), \tag{3}$$

with the following expressions for the terms:

$$\begin{aligned}
\boldsymbol{u}_j^n &= [\rho_j^n, v_j^n]^T, \\
\boldsymbol{F}(\boldsymbol{u}_j^n) = \boldsymbol{F}_j^n &= \left[\rho_j^n v_j^n, \frac{(v_j^n)^2}{2}\right]^T, \\
\boldsymbol{F_2}_j^n &= \left[\rho_j^n v_j^n, \frac{(v_j^n)^2}{2} + c_0^2 log(\rho_j^n)\right]^T, \\
\boldsymbol{g}_j^n &= \left[0, -\frac{c_0^2}{\rho_j^n h}(\rho_{j+1}^n - \rho_j^n) + \frac{\mu}{\rho_j^n h^2}(v_{j+1}^n - 2v_j^n + v_{j-1}^n)\right]^T, \\
\boldsymbol{g_2}_j^n &= \left[0, \frac{\mu}{\rho_j^n h^2}(v_{j+1}^n - 2v_j^n + v_{j-1}^n)\right]^T, \\
\boldsymbol{s}_j^n &= \left[q(t)\phi(x), \frac{1}{\tau}(V(\rho_j^n) - v_j^n)\right]^T.
\end{aligned} \tag{4}$$

Even though the pressure-term is derivated with respect to space, and thus should fit in $\boldsymbol{F}$, we have discovered that the antiderivative will give unstable algorithms for some of our methods, and we have chosen to differentiate it as a part of $\boldsymbol{g}$, either with forward difference or central difference depending on the method.

Lax-Friedrichs

The first method we implemented is Lax-Friedrichs, which is a one-step Lax-method. It is based on central differences in space and forward differences in time. We have tried adding the pressure term to the conservation term $\boldsymbol{F}$, but as the performance was approximately equal to the method we have used and the stability condition exactly equal, we chose the method resulting in a more generalized code.

$$\frac{\boldsymbol{u}_j^{n+1} - \frac{\boldsymbol{u}_{j+1}^n + \boldsymbol{u}_{j-1}^n}{2}}{k} = -\frac{\boldsymbol{F_2}_{j+1}^n - \boldsymbol{F_2}_{j-1}^n}{2h} + \boldsymbol{g_2}_j^n + \boldsymbol{s}_j^n$$

$$\boldsymbol{u}_j^{n+1} = \frac{\boldsymbol{u}_{j+1}^n + \boldsymbol{u}_{j-1}^n}{2} - \frac{\Delta t}{2h}(\boldsymbol{F_2}_{j+1}^n - \boldsymbol{F_2}_{j-1}^n) + k\boldsymbol{g_2}_j^n + k\boldsymbol{s}_j^n \tag{5}$$

Upwind

The second method we implemented is the Upwind method, which simulates the direction of propagation of information in a flow field. The method is based on forward difference in time and backward/forward difference in space depending on some conditions. We found out that the scheme was more stable with backward difference of $\boldsymbol{F}$ and forward difference for $\boldsymbol{g}$ with our equations and input-values.

$$\frac{\boldsymbol{u}_j^{n+1} - \boldsymbol{u}_j^n}{k} = -\frac{\boldsymbol{F}_j^n - \boldsymbol{F}_{j-1}^n}{h} + \boldsymbol{g}_j^n + \boldsymbol{s}_j^n$$

$$\boldsymbol{u}_j^{n+1} = \boldsymbol{u}_j^n - \frac{k}{h}(\boldsymbol{F}_j^n - \boldsymbol{F}_{j-1}^n) + k\boldsymbol{g}_j^n + k\boldsymbol{s}_j^n \tag{6}$$

Lax-Wendroff

We have implemented a two-step Lax-Wendroff method called Richtmyer, which is computing a solution a half step forward in time and space, and then using central difference around the half-step solution.

$$\begin{aligned} \boldsymbol{u}_{j+\frac{1}{2}}^{n+\frac{1}{2}} &= \frac{1}{2}\Big[\boldsymbol{u}_{j+1}^n + \boldsymbol{u}_j^n - \frac{k}{h}(\boldsymbol{F_2}_{j+1}^n - \boldsymbol{F_2}_j^n) \\ &\qquad + k\boldsymbol{g_2}_j^n + \frac{k}{2}(\boldsymbol{s}_{j+1}^n + \boldsymbol{s}_j^n)\Big], \\ \boldsymbol{u}_j^{n+1} &= \boldsymbol{u}_j^n - \frac{k}{h}\Big[\boldsymbol{F_2}_{j+\frac{1}{2}}^{n+\frac{1}{2}} - \boldsymbol{F_2}_{j-\frac{1}{2}}^{n+\frac{1}{2}}\Big] + k\boldsymbol{g_2}_{j+\frac{1}{2}}^{n+\frac{1}{2}} \\ &\qquad + \frac{k}{2}\Big[\boldsymbol{s}_{j+\frac{1}{2}}^{n+\frac{1}{2}} + \boldsymbol{s}_{j-\frac{1}{2}}^{n+\frac{1}{2}}\Big]. \end{aligned} \tag{7}$$

MacCormack

MacCormack is a two-step extension of the Lax-Wendroff scheme, based on first doing a predictor step and then a corrector step for a more accurate discretization. The predictor step is equal to the first order Upwind method, using mainly backward finite difference approximation for spatial derivative. The corrector step corrects the approximated value $\tilde{\boldsymbol{u}}_j^n$, by averaging between the predictor and a downwind step calculated with the predicted value. The method can also be implemented with downwind as the predictor step, and Upwind as the corrector, but we have chosen using Upwind first based on our experiences with what gives the most stable Upwind scheme.

$$\begin{aligned} \tilde{\boldsymbol{u}}_j^n &= \boldsymbol{u}_j^n - \frac{k}{h}(\boldsymbol{F}_j^n - \boldsymbol{F}_{j-1}^n) + k\boldsymbol{g}_j^n + k\boldsymbol{s}_j^n, \\ \boldsymbol{u}_j^{n+1} &= \frac{1}{2}\Big[\tilde{\boldsymbol{u}}_j^n + \boldsymbol{u}_j^n - \frac{k}{h}(\tilde{\boldsymbol{F}}_{j+1}^n - \tilde{\boldsymbol{F}}_j^n) + k\tilde{\boldsymbol{g}}_j^n + k\tilde{\boldsymbol{s}}_j^n\Big]. \end{aligned} \tag{8}$$

Boundary and initial conditions

In order to simulate the equations, we need to have some boundary conditions. In our implementation we have looked at a road of length $L = 5000$ m, which is discretized into $M = 2^{12}$ space points. Setting $\rho(-L/2, t) = \rho_0$ and $v(-L/2, t) = V(\rho_0)$ gives reasonable results, but if the queue starts to accumulate and the density near $-L/2$ increases, we would get a large jump in density from $\rho(-L/2, t)$ to $\rho(-L/2 + h, t)$ and similarly a decrease in the velocity. Although we have not seen any large impact on the results, we wanted to find a more accurate $\rho(-L/2, t)$. Our solution is to set $\rho(-L/2, t) = \rho(-L/2 + h, t - k)$ and $v = V(\rho(-L/2 + h, t - k))$ which does not give the large jumps in density and velocity between the two first spatial steps.

For the other boundary condition, at L/2, we use extrapolation from the values at $(L/2 - h)$ and $(L/2 - 2h)$ to compute $\rho(L/2, t)$ and $v(L/2, t)$.

Further, the following parameters are chosen: $\tau = 30$ s, $\mu = 0$ vehicles m/s, $c_0 = 15$ m/s, $V(\rho) = V_0(1 - \rho/\rho_{max})/(1 + E(\rho/\rho_{max})^4)$ m/s, where $\rho_{max} = 0.140$ vehicles/m is the maximum density, $V_0 = 33.33$ m/s and $E = 100$. We have used the incoming rate at the on-ramp

$$q(t) = \begin{cases} 0.1 & t < 30 \\ 0 & t \geq 30, \end{cases}$$

which is normally distributed,

$$\varphi(x) = \frac{e^{-x^2/2\sigma^2}}{\sqrt{2\pi\sigma^2}}$$

with $\sigma = 300$ m.

Results and applications

The traffic equations can be used to model how traffic behaves around an on-ramp. Figure 1, 2, **??** and 3 shows how the traffic behaves using different functions for $q_{in}(t) = 0.5$ for $t < 30$ and $q_{in}(t)$ otherwise. With our input, queues seems to move backwards on the roads, which is natural if cars use longer time to accelerate out of the queue than breaking when approaching the queue. Other inputs does however result in a queue moving forwards (at least one of the other groups have this solution, which we also get with the same inputs). Another interesting thing we see in our plots is that density tends to go down ahead of the queue, resulting in higher velocities. The post-queue-velocities works locally, but are too high for the overall density on the road, which results in new queues further down the road. Thus these queues end up moving forwards and

backwards, and we get low-density and high-density areas on the road, even though we turn off the on-ramp. This behavior fits well with so-called shockwave traffic jams, or phantom traffic jams.

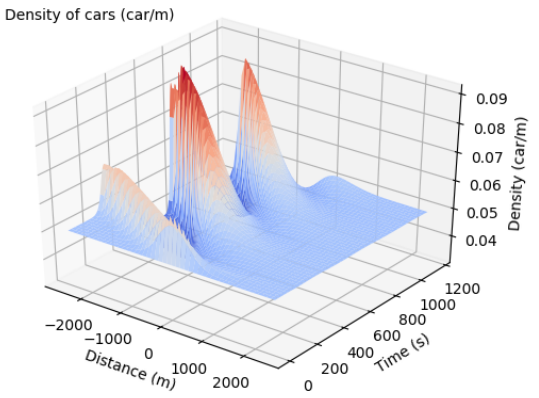

Figure 1: Plot showing development in time for the density of cars using the Upwind scheme, and $h = 100$ and $k = 0.05$.

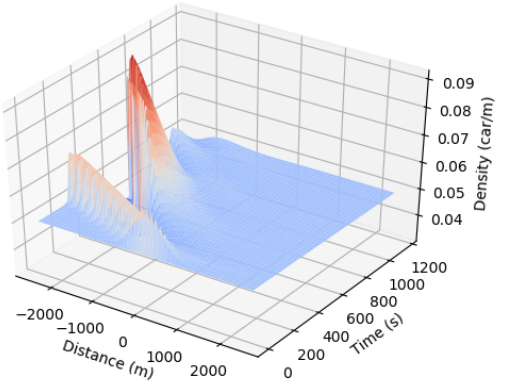

Figure 2: Plot showing development in time for the density of cars using the Lax-Friedrich scheme, and $h = 5$ and $k = 0.1$.

Note also the difference in figure 1 and 2. In the beginning, they are very similar but as time develops, the queue seems to disappear for Lax-Friedrich, while the queues does not disappear for Upwind. Thus, as time goes, the solutions become very different. We know Lax-Friedrich suffers from dissipation error, and although this error is small in the beginning, it seems to develop over time, resulting in the queue disappearing. We will discuss this amplitude difference further in the convergence-section.

Figure 4 shows solutions from the Lax-Wendroff scheme. The solutions are quite similar to the lax-Friedrichs scheme, though the solution seems to start oscillate eventually. The Lax-Wendroff scheme is in general quite

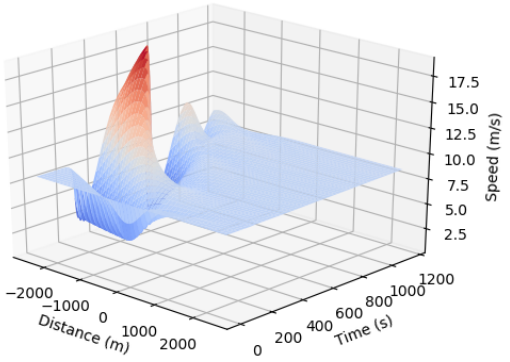

Figure 3: Plot showing development in time for the velocity of cars using the Lax-Friedrich scheme, and $h = 5$ and $k = 0.1$.

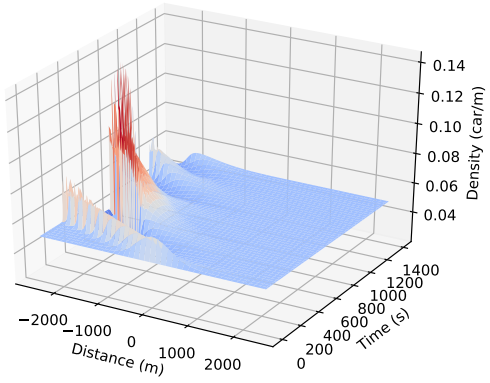

Figure 4: Plot showing the density ρ using the Lax-Wendroff scheme. The solution is plotted for $k = 1.4$ sec and $h = 39.3$ m.

unstable, and we have to be very careful with input values to get solutions at all.

It is also worth mentioning that as we have set $\mu = 0$ in our implementations, the dampening term in (2) makes no impact. The reason why μ has been given this value, is because it is difficult to obtain stable results for the different schemes when this term is taken into account. It is thus also difficult to compare convergence of the different schemes when we include this term. However, for the Upwind scheme it works well to have $\mu \neq 0$. In figure 5, we see that the results are much smoother when $\mu = 150$ and the dampening effect thus is included.

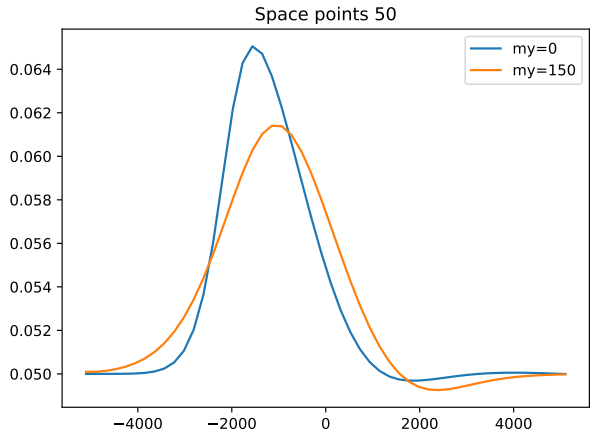

Figure 5: Plot showing the density ρ after 100 seconds using the Upwind scheme. The solution is plotted for respectively $\mu = 0$ and $\mu = 150$.

Analysis

Consistency

A method for solving a partial differential equation is consistent if the truncation error approaches zero as the time step k and the spatial step h goes towards zero. The truncation error of the different schemes can be found by Taylor expansions. In the Lax-Friedrichs discretization of the traffic equations, we have to Taylor expand the terms $\rho_j^{n+1}, \rho_{j+1}^n, \rho_{j-1}^n, v_j^{n+1}, v_{j+1}^n$ and v_{j-1}^n. The second order Taylor expansions of these terms are

$$\rho_j^{n+1} = \rho(x_j, t_n) + k\rho_t(x_j, t_n) + \frac{k^2}{2}\rho_{tt}(x_j, t_n) + \mathcal{O}(k^3), \tag{9}$$

$$\rho_{j+1}^n = \rho(x_j, t_n) + h\rho_x(x_j, t_n) + \frac{h^2}{2}\rho_{xx}(x_j, t_n) + \mathcal{O}(h^3), \tag{10}$$

and

$$\rho_{j-1}^n = \rho(x_j, t_n) - h\rho_x(x_j, t_n) + \frac{h^2}{2}\rho_{xx}(x_j, t_n) + \mathcal{O}(h^3). \tag{11}$$

For the v-terms, the Taylor series are similar. When inserting these into the Lax-Friedrichs scheme (5), and moving all the terms to one side, we get for equation (1)

$$\begin{aligned}
\tau_j^n = \frac{1}{k}\Big(&\rho_j^n + k\rho_t + \frac{k^2}{2}\rho_{tt} + \mathcal{O}(k^3)\Big) \\
&-\frac{1}{2k}\Big(\rho_j^n + h\rho_x + \frac{h^2}{2}\rho_{xx} + \mathcal{O}(h^3) \\
&+\rho_j^n - h\rho_x + \frac{h^2}{2}\rho_{xx} + \mathcal{O}(h^3)\Big) \\
&+\frac{v_j^n}{2h}\Big(\rho_j^n + h\rho_x + \frac{h^2}{2}\rho_{xx} + \mathcal{O}(h^3) \\
&-\big(\rho_j^n - h\rho_x + \frac{h^2}{2}\rho_{xx} + \mathcal{O}(h^3)\big)\Big) \\
&+\frac{\rho_j^n}{2h}\Big(v_j^n + hv + \frac{h^2}{2}v_{xx} + \mathcal{O}(h^3) \\
&-\big(v - hv + \frac{h^2}{2}v_{xx} + \mathcal{O}(h^3)\big)\Big) - q(t)\phi(x),
\end{aligned} \tag{12}$$

where $\rho, \rho_t, \rho_{tt}, \rho_x$ and ρ_{xx} all are evaluated in (x_j, t_n). This can further be simplified to

$$\begin{aligned}
\tau_j^n = \rho_t + v\rho_x + \rho v_x - q(t)\phi(x) + \\
\frac{k}{2}\rho_{tt} + \mathcal{O}(k^2) + \frac{h^2}{2k}\rho_{xx} + (\frac{1}{k} + \frac{v}{2h} + \frac{\rho}{2h})\mathcal{O}(h^3).
\end{aligned} \tag{13}$$

$\rho_t + v\rho_x + \rho v_x - q(t)\phi(x)$ can be set equal zero, as this is the original equation. In addition, if the stability criterion, discussed in the stability section, is fulfilled, we have that $k = \mathcal{O}(h)$. Thus, we end up with

$$\tau_j^n = \mathcal{O}(k) + \mathcal{O}(k^2) + \frac{\mathcal{O}(h^2)}{k} + \mathcal{O}(h^2) = \mathcal{O}(k) + \mathcal{O}(h). \tag{14}$$

We get the same results using the same calculations on the second equation. In other words, the Lax-Friedrichs scheme for this equation is consistent and of first order accuracy in both space and time.

For the Upwind scheme, we obtain the same result by following exactly the same procedure. Thus, we also have first order accuracy in both space and time also for this method.

The truncation errors for Lax-Wendroff and MacCormack have not been calculated by hand. The order of accuracy of these schemes will be discussed in the numerical justification part later on.

Stability

We also want to investigate stability for our difference schemes. One way to do this is by performing Von Neumann-analysis. Since the traffic equations are a set of nonlinear equations, we will linearize the equations, since Von Neumann-analysis can become rather unappetizing with non-linear equations.

Linearization

We will also for the stability-analysis turn off the on-ramp ($q_{in}(t) = 0$)),to simplify the analysis. We now observe that $\rho = c_1$ and $v = c_2$, with c_1 and c_2 as constants, are solutions to equation (1) with $q_{in}(t) = 0$. Furthermore, if we set $c_2 = V(c_1)$, the first term on the right hand side in equation (2) becomes zero, making these choices for ρ and v solutions to equation (2) as well. For the linearization, we define

$$u = [\rho, v]^T = [\bar{\rho} + \epsilon r, \bar{v} + \epsilon s]^T. \tag{15}$$

Here, $\bar{\rho}$ and $\bar{v}$ must be known solutions to our equations, and the constant solutions discussed above will do just fine. Hence $\bar{\rho}$ is a constant, and $\bar{v} = V(\bar{\rho})$, which is also a constant. Inserting (15) into (1) gives

$$\begin{aligned} 0 = (\bar{\rho} + \epsilon r)_t + ((\bar{\rho} + \epsilon r)(\bar{v} + \epsilon s))_x = \\ \bar{\rho}_t + (\bar{\rho}\bar{v})_x + \epsilon(r_t + \bar{v}r_x + \bar{\rho}s_x) + \epsilon^2(rs)_x \end{aligned} \tag{16}$$

Similarly, inserting (15) into (2) gives

$$\begin{aligned} &0 = (\bar{v} + \epsilon s)_t + (\bar{v} + \epsilon s)(\bar{v} + \epsilon s)_x \\ &+ c_0^2 \frac{(\bar{\rho} + \epsilon r)_x}{(\bar{\rho} + \epsilon r)} - \mu \frac{(\bar{v} + \epsilon s)_{xx}}{(\bar{\rho} + \epsilon r)} \implies \\ &0 = \frac{(\bar{\rho} + \epsilon r)}{\bar{\rho}}(\bar{v}_t + \bar{v}\bar{v}_x + c_0^2 \frac{\bar{\rho}_x}{(\bar{\rho} + \epsilon r)} - \mu \frac{\bar{v}_{xx}}{(\bar{\rho} + \epsilon r)} \\ &+ \epsilon(s_t + \bar{v}s_x + s\bar{v}_x + c_0^2 \frac{r_x}{(\bar{\rho} + \epsilon r)} - \mu \frac{s_{xx}}{(\bar{\rho} + \epsilon r)}) + \epsilon^2(rs)_x) \end{aligned} \tag{17}$$

By ignoring terms with ϵ^2 and higher, we get a new system of linear equations:

$$r_t + \bar{v}s_x + \bar{\rho}s_x = 0 \tag{18}$$

$$s_t + \bar{v}s_x + \frac{c_0^2}{\bar{\rho}} r_x - \frac{\mu}{\bar{\rho}} s_{xx} = 0 \tag{19}$$

We will then proceed by doing von Neumann analysis on these linearized equations.

Von Neumann analysis

After the linearization we get the following expressions for the terms in (4), with the source/sink term $\boldsymbol{s_j^n} = 0$ from the assumptions made in the linearization.

$$\begin{aligned} &\boldsymbol{u}_j^n = [r_j^n, s_j^n]^T, \\ &\boldsymbol{F}_j^n = \left[\bar{v}r_j^n + \bar{\rho}s_j^n, \frac{c_0^2}{\bar{\rho}} r_j^n + \bar{v}s_j^n\right]^T = A\boldsymbol{u}_j^n = \begin{bmatrix} \bar{v} & \bar{\rho} \\ \frac{c_0^2}{\bar{\rho}} & \bar{v} \end{bmatrix} \boldsymbol{u}_j^n, \\ &\boldsymbol{g_2}_j^n = \left[0, \frac{\mu}{\bar{\rho}h^2}(s_{j+1}^n - 2s_j^n + s_{j-1}^n)\right]^T, \end{aligned} \tag{20}$$

Inserting these new terms into the numerical schemes and introducing the eigenmode as $\boldsymbol{u}_j^{n+1} = \xi^{n+1} e^{i\theta j}\boldsymbol{u}_0$, we can solve the equations for ξ and use the Von Neumann stability criterion, $|\xi|^2 \leq 1$, to find the values of h and k so that the methods are stable. The following calculations are for Lax-Friedrichs and the results are for Lax-Friedrichs and Upwind. The procedure will be the same for all our methods, but we have not done this for Lax-Wendroff and MacCormack.

$$\begin{aligned} \xi^{n+1} e^{i\theta j}\boldsymbol{u}_0 = \\ &\frac{\xi^n}{2}(e^{i\theta(j+1)} + e^{i\theta(j-1)})\boldsymbol{u}_0 \\ &- \frac{\xi^n k}{2h} A(e^{i\theta(j+1)} - e^{i\theta(j-1)})\boldsymbol{u}_0 \\ &+ \xi^n k \begin{bmatrix} 0 & 0 \\ 0 & \frac{\mu(e^{i\theta(j+1)} - 2e^{i\theta j} + e^{i\theta(j-1)})}{\bar{\rho}h^2} \end{bmatrix} \boldsymbol{u}_0 \end{aligned} \tag{21}$$

Dividing by $\xi^n e^{i\theta j}$ and using trigonometric identities, we get

$$M\boldsymbol{u}_0 = \begin{bmatrix} -\xi + \cos(\theta) & -\frac{k\bar{\rho}}{h} i\sin\theta \\ -\frac{k\bar{v}}{h} i\sin\theta & -\xi + \cos(\theta) - \frac{k\bar{v}}{h} i\sin\theta + \frac{2\mu(\cos(\theta) - 1)}{\bar{\rho}h^2} \\ -\frac{kc_0^2}{h\bar{\rho}} i\sin\theta & \end{bmatrix} \begin{bmatrix} r_0 \\ s_0 \end{bmatrix} = \begin{bmatrix} 0 \\ 0 \end{bmatrix} \tag{22}$$

To get non-trivial solutions for (22), we solve $\det(M) = 0$. This results in the following solution for ξ:

$$\begin{aligned} \xi = \cos(\theta) - \frac{\mu k}{\bar{\rho}h^2}(1 - \cos(\theta)) \\ -\bar{v}\frac{k}{h} i\sin\theta \pm \frac{k}{h^2}\sqrt{\frac{\mu}{\bar{\rho}}^2 (1 - \cos(\theta))^2 - c_0^2 \sin^2(\theta)} \end{aligned} \tag{23}$$

With $\mu = 0$ we obtain an expression for $\frac{k}{h}$:

$$\begin{aligned} \textbf{Lax-Friedrichs:} \quad |\xi|^2 \leq 1 \\ \implies \frac{k}{h}(\bar{v} + c_0) \leq 1 \end{aligned} \tag{24}$$

$$\begin{aligned} \textbf{Upwind:} \quad \left[1 - \frac{k\bar{v}}{h}(1 - \cos(\theta))\right]^2 \\ + \frac{k}{h}^2 \left[-\sin(\theta)\bar{v} \pm c_0\sqrt{1 - \cos(\theta)}\right]^2 \leq 1 \end{aligned} \tag{25}$$

Convergence

According to Lax' equivalence theorem [2], consistency and stability as we have shown here implies conver-

gence for one-step schemes as Lax-Friedrichs and Upwind. However, for multistep schemes, this is not necessarily the case and the convergence analysis for these schemes is a bit more complicated.

Numerical justification

Stability conditions

From the stability analysis, we have found conditions that must be satisfied in order to expect stable solutions. Due to the linearization and other simplifications, we do not expect the stability conditions to work perfectly with our equations. Still, the stability conditions should be a good indicator on when we get stable solutions. For our solutions, we use $\rho_0 = 0.05$. This is the equivalence of $\bar{\rho} = 0.05$, resulting in $\bar{v} = V(0.05) = 8.16$ m/s. Also we have $c_0 = 15$ m/s. For these values, equation (24) is valid for $k/h < 0.043$. Using our Lax-Friedrichs-scheme, we observe stable solutions for $k/h < 0.05$ when running shorter periods of time. It is possible running for longer time will eventually result in unstable solutions, but it seems to fit well with the analysis. For Upwind, it is not quite easy to see the stable conditions for equation (25), but using calculation programs, we find the conditions to hold for $k/h < 0.023$. Running our Upwind scheme, we find stable solutions for $k/h < 0.021$. Thus, we get unstable solutions for values which should be okay according to the analysis. This might be explained by the choice of a constant $\bar{\rho}$, which is not really the case for our simulations. Using the on-ramp, the density becomes higher, resulting in a lower v. If we use a lower value for $\bar{v}$ in the analysis, we do indeed see stricter stability conditions. This might explain why we require a stricter stability condition than the analysis shows. In any case, they are quite close, showing that the analysis fits our implementation quite well.

Convergence plots

In figure 6 and 7, the error of our methods compared to a reference solution as function of the time step used, is plotted for respectively ρ and v. Note however that they all converge towards a more exact solution with respect to their own scheme. We have here used $h = 19.5$ m. From the consistency analysis, we expect the Lax-Friedrichs and Upwind schemes to have first order convergence in both space and time. Figure 6 and 7 seems to be in agreement with this, especially for Lax-Friedrichs. Upwind have a slope of almost 1.5, which is higher than the theoretical order found in the consistency analysis. A reason for this may be the boundary conditions given in our implementation. The Lax-Wendroff and MacCormack methods look here like having the same convergence order as Upwind. As we have not calculated the truncation errors of these schemes by hand, it is difficult to say whether these methods theoretically have first order convergence or not for our equations. In general, the two-step Lax-Wendroff and MacCormack methods for linear equations tend to have second order accuracy in both time and space [3] [4] [5], so this is perhaps what we would have expected before obtaining these convergence plots. However, as we have a non-linear equation, it is possible that the properties of our equation gives an order reduction.

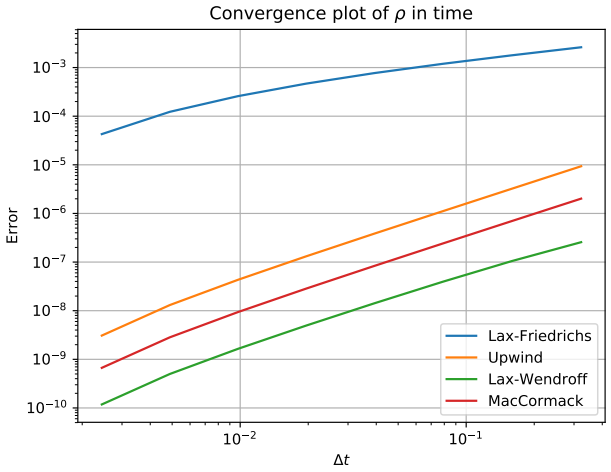

Figure 6: Plot showing the convergence order of ρ in time for the different methods.

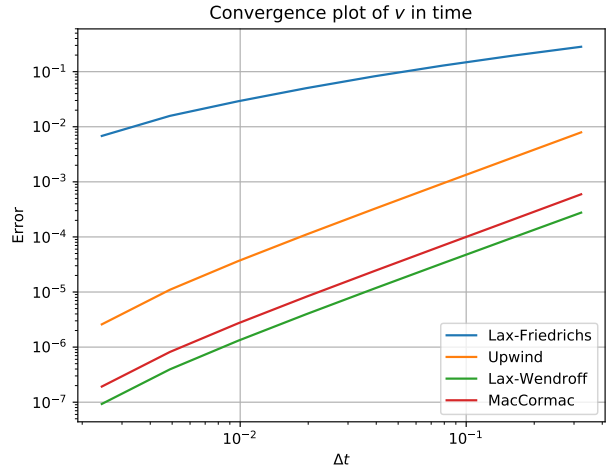

Figure 7: Plot showing the convergence order of v in time for the different methods.

Figure 8 shows time convergence where they all converge towards the same reference solution, made with the Upwind scheme. The error is generally very low, and all schemes but one converges to zero. They therefore seem to converge towards the same solution, which makes the implementation seem correct. Lax-Friedrichs is the exception, and although it is similar, it seems to

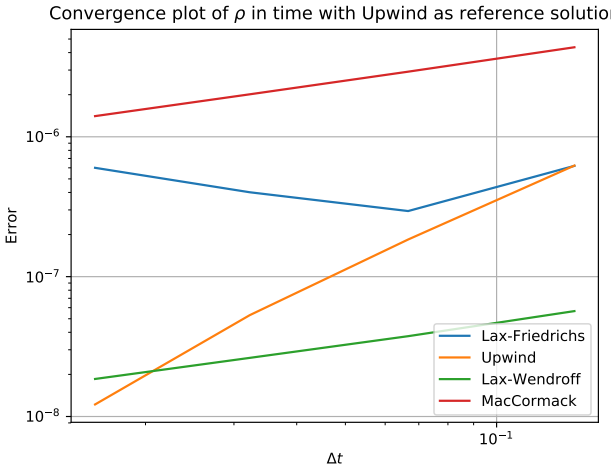

Figure 8: Plot showing the convergence order of v in time for the different methods, with the Upwind method as the "exact" solution.

go towards the Upwind-solution, and then pass it by and continue towards some other solution. This illustrates the dissipation problem: if k/h becomes too small, we see that Lax-Friedrichs converges to a different solution, where the amplitude is too low. By decreasing kt without changing h, Lax-Friedrichs converges towards the wrong solution, and although the error is small, this can develop in time, making quite different solutions, as discussed earlier.

Looking at figure 9 and 10, we see the error for ρ and v as a function of step size h in space. The error has not been plotted over the same interval of step sizes for all the methods, as the Upwind and Lax-Wendroff schemes must have really small time steps k compared to space steps h in order to remain stable. They also seem to converge better when the simulations of the model are run for a duration around a minute. The Lax-Friedrichs scheme on the other hand demands a step size in space smaller than 10 m in order to converge. This is probably due to the dissipation error that Lax-Friedrichs suffer from. When the step size is too large, this method has solutions with too low amplitude, and it does not start to converge until the spatial step size is sufficiently small. MacCormack is the only scheme which seem to converge on the whole interval we have evaluated.

Conclusion

In this project, we have investigated the traffic equations (1) and (2). Four different finite difference discretization methods have been implemented for our equations, respectively the one-step schemes Lax-Friedrichs and Upwind and the two-step schemes Lax-Wendroff and MacCormack. From the results obtained and analysis made,

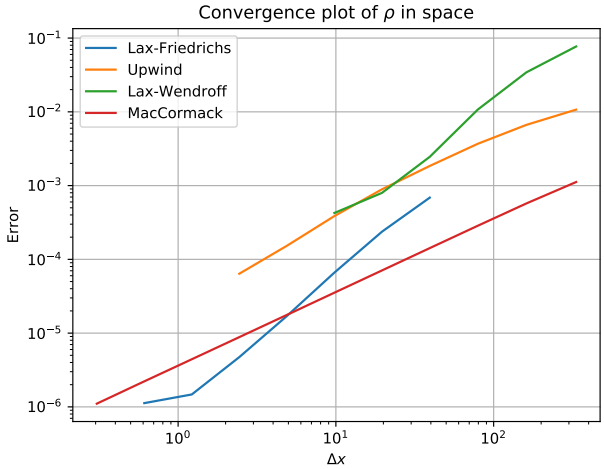

Figure 9: Plot showing the convergence order of ρ and v in space for the different methods.
Lax-Friedrichs: time: 1 sec, timepoints: 1000,
Upwind: time: 40 sec, timepoints: 2000,
Lax-Wendroff: time: 160 sec, timepoints: 1000,
MacCormack: time: 1 sec, timepoints: 1000

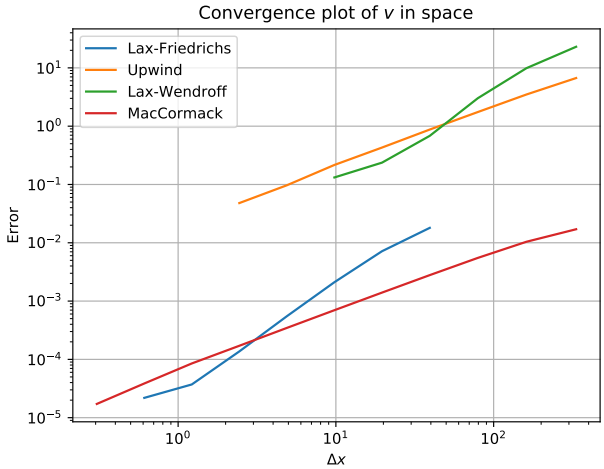

Figure 10: Plot showing the convergence order of v in time for the different methods. The same values for time and timepoints as in figure 9 is used

Lax-Friedrichs seems to be quite stable, as the stability region found is much less strict than the one for Upwind. However, if the ratio between the time step and the space step is too small, we get dissipative effects. The Upwind method also works well inside its stability region. The Lax-Wendroff and MacCormack schemes have not been analyzed to the same extent as the one-step methods, but Lax-Wendroff tends to be a bit more unstable than MacCormack. We have also verified our methods through convergence plots in time and space, showing the order of convergence for the different methods.

All the group members have contributed equally to the project work.

References

[1] Lee, H.Y., Lee, H.-W., Kim, D. *Dynamic states of a continuum traffic equation with on-ramp*, https://journals.aps.org/pre/pdf/10.1103/PhysRevE.59.5101 (1999)

[2] Owren, B. *TMA4212 Numerical solution of partial differential equations with finite difference methods*, (2017)

[3] Rezzolla, L. *Numerical Methods for the Solution of Partial Differential Equations*, http://www.aei.mpg.de/ rezzolla/lnotes/Evolution_Pdes/evolution_pdes_lnotes.pdf (2011)

[4] Hudson, J. *Numerical Techniques for Conservation Laws with Source Terms*, https://www.reading.ac.uk/web/files/maths/J_Hudson.pdf (2011)

[5] Fennema, R.J., Chaudhry, M.H. *Explicit Numerical Schemes for Unsteady Free-Surface Flows With Shocks*, https://agupubs.onlinelibrary.wiley.com/doi/pdf/10.1029/WR022i013p01923 (1986)

[6] Helbing, D., Treiber, M. *Numerical Simulation of Macroscopic Traffic Equations*, https://arxiv.org/pdf/cond-mat/9909033.pdf (1999)

[7] Press W.H., Teukolsky, S.A., Vetterling, V.T., Flannery, B.P. *Numerical Recipes in C*, https://www2.units.it/ipl/students_area/imm2/files/Numerical_Recipes.pdf (2002)